Theoretical Analysis of the Spunbond Process and its Applications for Polypropylenes

Toshitaka Kanai[1,a)*], Youhei Kohri[2,b)], Tomoaki Takebe[2,c)]

[1] *KT Polyme: 5-7-14 Kuranamidai, Sodegaura, Chiba, Japan*
[2] *Performance Materials Laboratories, Idemitsu Kosan Co., Ltd. Anesaki, Ichihara ,Chiba, Japan*

[a)]Corresponding author: toshitaka.kanai@ktpolymer.com
[b)] yohei.koori@idemitsu.com, [c)] tomoaki.takebe@idemitsu.com

Abstract: The theoretical analysis of the spunbond process was set up and applied to polypropylene (PP) and its blends. The effect of blending low tacticity polypropylene (LMPP) to high tacticity PP on the spinnability of the spubond process was investigated. A small amount of LMPP was found to stabilize the high speed spinning of PP and very fine fibers were obtained. From the calculated results, it was speculated that the improvement of spinnability originated from the suppression of crystallization speed and strain rate in the spinning process. Physical properties of spunbond nonwoven fabrics were also investigated.

1. INTORODUCTION

The spunbond non-woven fabrics are widely used for disposal diapers. They are required to be soft and composed of fine fibers. Our previous research found that the blending of a small amount of low tacticity polypropylene (LMPP) to commercial high tacticity polypropylene (PP) could produce very fine fiber without breaking under high speed spinning conditions[1)-5)]. Furthermore, this blend was also applicable for the PP spunbond process and highly improved spinnability. It was surmised that these results came from the retardation of crystallization speed of PP and the prevention of quick deformation during the spinning process by adding LMPP [4),5)].

The theoretical analysis during the spunbond process was formulated and applied for the blends of LMPP to PP in order to investigate the deformation behavior during the spunbond process.

2. THEORETICAL ANALYSIS OF SPUNBOND PROCESS

In order to set up the theoretical equations of the spunbond process shown in Figure 1, several assumptions were made as follows.

① The cross section of the fiber was round and axi-symmetric
② Heat conduction along the axis was not considered because the spinning speed is very fast
③ The spinning line was treated as being in the steady state
④ The swell was assumed to be constant
⑤ The elongational viscosity of the polymer is as a function of temperature and crystallinity. The temperature dependence of viscosity is followed by the Arrhenius type and the temperature is balanced between the crystallization heat and the air cooling during the region of crystallization. The crystallization temperature is assumed to be the same as the crystallization temperature obtained by DSC data. After the latent heat ΔH was consumed the temperature decreases.
⑥ The temperature distribution along the radius direction was neglected and the heat transfer was only considered from the surface. The x axis was taken in the center along the spinning axis.

Under the above conditions, momentum equation (1), continuity equation (2), energy equation (3) and rheological equation (4) with the help of boundary conditions were used to solve the spinning behavior by using the Runge-Kutta Verner method. The boundary conditions were fiber temperature, fiber speed and cross sectional area at the die exit. The spunbond process which was different from melt spinning did not

have a winder, so the final spinning speed and take-up force at the entrance of channel in a chamber are unknown. Therefore, an arbitrary force was used at first and then the spinning force at the entrance of the channel in a chamber which was obtained by solving the above equations along the spinning line was compared with the friction force induced on the fiber surface in the channel. By using the Newton Raphson method, an appropriate value was determined by obtaining the same values between the spinning force at the entrance of the channel and the friction force induced on the fiber surface in the channel. These procedures gave the diameter distribution, spinning speed distribution, deformation rate distribution, fiber temperature and spin line force.

$$\frac{dF}{dx} = W\left(\frac{dv}{dx} - \frac{g}{v}\right) + \pi D\tau_f = W\left(\frac{dv}{dx} - \frac{g}{v}\right) + 0.0023(Av^2)^{0.195}v \quad (1)$$

$$\frac{dA}{dx} = -\frac{A}{v}\frac{dv}{dx} \quad (2)$$

$$\frac{dT}{dx} = -\left(\frac{2\pi A}{C_p W}\right)h(T - T_{air}) \quad (3)$$

$$\frac{dv}{dx} = \frac{F}{3\eta_0 A}exp\left[-\frac{E}{R}\left(\frac{1}{T} - \frac{1}{T_0}\right) + GX\right] \quad (4)$$

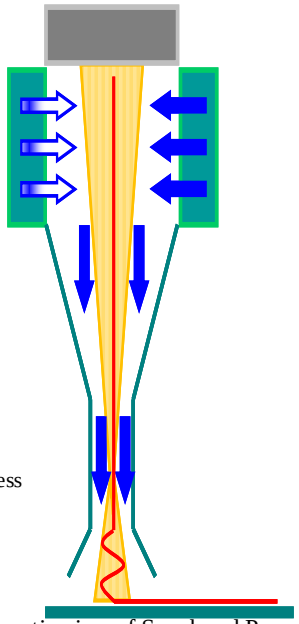

FIGURE 1. Schematic view of Spunbond Proocess

F : spinning force, W : Out-put rate per nozzle, g : gravity accelaration, τ_f : air friction stress
A : cross section of fiber, v : spinning speed, D : fiber diameter,
h : heat transfer coefficient, Cp : specific heat, η_0 : zero-shear viscosity,
E : activation energy of melt resin viscosity, T : fiber temperature,
T_{air} : cooling air temperature, T_0 : resin temperature at the nozzle exit,
G : viscosity rising-index of crystallization (PP 100%;1.0, PP/ LMPP10%;0.8, PP/ LMPP20%;0.6), X : crystallinity

$$F_{x=L} = \alpha\left[\frac{(v_{air} - v)D}{v^*}\right]^{\gamma}(v_{air} - v)^2\frac{\rho^*}{2}\pi DL \quad (5)$$

α : air friction coefficient, v_{air} : cooling air speed at the narrow channel in the cabin, ρ^* : air density,
D : final fiber diameter at the narrow channel in the cabin, v^* : air kinematic viscosity, L : length the narrow channel in the cabin

3. RESULTS AND DISCUSSION

3.1 The Blending Effect of LMPP to PP for Spinnability of Spunbond Non-woven Process

The high tacticity PP (PP Exxon3155 produced by ExxonMobil, MFR=36g/10min, T_m=160℃) 100% and the blends of 10wt% -15wt% LMPP (LMPP produced by Idemitsu Kosan) to high tacticity PP were used. LMPP (LMPP1, MFR=50g/10min, T_m=75℃ ; LMPP2, MFR=600g/10min, T_m=75℃) were polymerized by using a single site catalyst. The blends of LMPP 10wt % or 15wt % (LMPP1-10%,-15%、LMPP2-15%) with high tacticity PP were used for the spunbond process.

The crystallization speed was evaluated by using Flash DSC (Mettler Toledo) at the high cooling speed 2,000℃/sec shown in Figure 2. IPP-100% had a half crystallization time of 0.066sec and LMPP1-10% had a half crystallization time of 0.094sec and addition of LMPP to PP decreased the crystallization speed of PP. The crystallization temperature and the latent heat Δ H shown in Figure 3 were obtained by Perkin Elmer DSC7. The spinnability was carefully observed for three minutes under various conditions and whether fiber breaks occurred was confirmed and then stable conditions which had no breaks were determined to be the stable conditions.

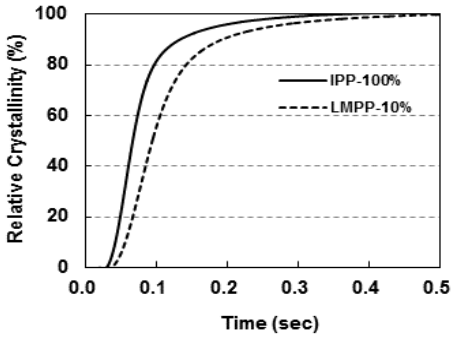

FIGURE 2. Time variation of relative crystallinity

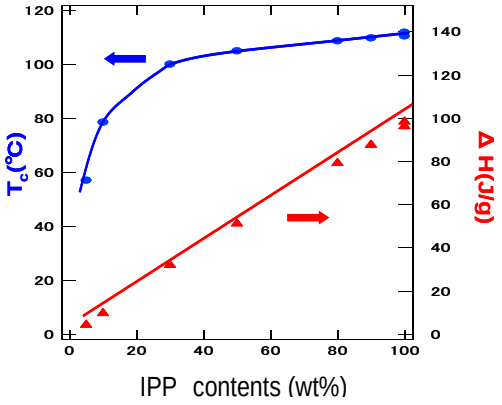

FIGURE 3 Tc and Δ H as a function of IPP

Table 1 shows the process conditions such as output rate, cabin pressure, spinning speed and minimum fiber diameter give maximum stable conditions for blends IPP-100% and LMPP-10%.

The stable conditions for IPP-100% was a throughput rate of 0.6g/min/hole, a cabin pressure of 4,500Pa and a fiber diameter of 1.7denier at the maximum spinning speed of 3,200m/min. On the contrary, the blends of LMPP1 10% with IPP could expand the stable condition area and produce fine fiber diameters of 1.1 denier at the maximum spinning speed of 4,200m/min, because of a lower maximum strain rate and less stress.

3.2 Spinning Behavior of Spunbond Process

The comparison of the predicted results with experimentally observed denier for the spunbond process is shown in Figure 4. This figure shows that the theoretical analysis of the spunbond process can predict the fiber diameter if the process conditions are input. Figures 5, 6 and 7 show the deformation behaviors such as fiber diameter, strain rates and stresses were predicted along the spin-line under PP-100 wt%, throughput 0.6g/min/hole and the various cabin pressures.

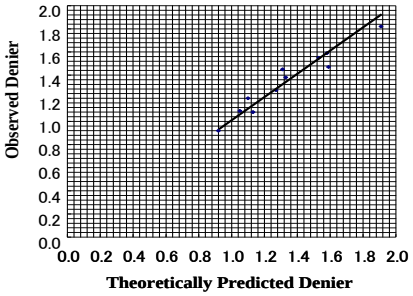

FIGURE 4 Comparison of predicted deniers with Experimentally observed for the spunbond process

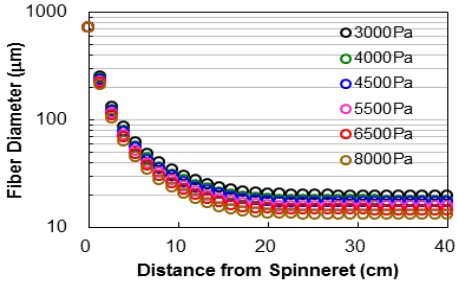

FIGURE 5 Fiber Diameter Distribution under different cabin pressures

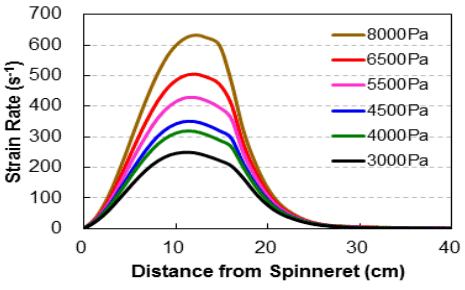

FIGURE 6 Strain rate under different cabin pressures

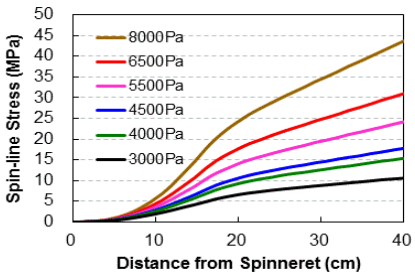

FIGURE 7 Stress under different cabin pressures

Spinning speed increases and fiber diameter decreases with increasing cabin pressure. The maximum strain rate and spinning stress increase with increasing cabin pressure. The cabin pressure strongly influences the deformation behavior. The throughput and the resin temperature are also important to control the denier of each fiber.

The effect of blending LMPP with PP on spinnability of the spunbond process was also investigated by solving the theoretical equations during the spunbond process. Figures 8, 9 and 10 show the fiber diameter, strain rate and stress profiles of PP and of the PP /LMPP 10% and 20% blends along the spin-line obtained by theoretical predictions under the same conditions as output rate 0.6g/min/hole and cabin pressure of 4,500Pa.

As the crystallization speed which was changed by G value of viscosity raising-index of crystallization can be reduced by adding LMPP, the fiber diameter gradually decreases along the spin-line. The maximum strain rate and stress decreases with increasing the LMPP content.

Furthermore, additional studies were done by changing LMPP content (0, 10, 15%) and LMPP molecular weight (MFR 50, 600). The maximum strain rate decreased by adding LMPP and the strain rate gradually decreased in the region of the downstream area. The rapid change of the strain rate during the spinning was suppressed by adding LMPP.

As Table 1 shows, it was concluded that the increase of maximum spinning speed for PP and LMPP blends originated from the suppression of crystallization speed of PP and the reduction of maximum strain rate in the spinning process. When the comparison between LMPP1-15% and LMPP2-15% which had different molecular weights was made, the lower viscosity of LMPP 2 could stably produce the finer fiber diameter under the higher cabin pressure and reach 0.9 denier.

Table 1. Fiber diameter and spinning velocity of various PP blends under the limited conditions of stable spinning.

Sample Code	Throughput (g/min/hole)	Cabin Pressure (Pa)	Fiber Diameter (denier)	Spinning Velocity (m/min)
IPP-100%	0.60	4,500	1.7	3,200
LMPP1-10%	0.60	6,500	1.4	3,900
	0.50	6,500	1.1	4,200
	0.40	5,500	1.1	3,300
LMPP1-15%	0.36	6,500	1.0	3,200
LMPP2-15%	0.36	6,500	0.9	3,800

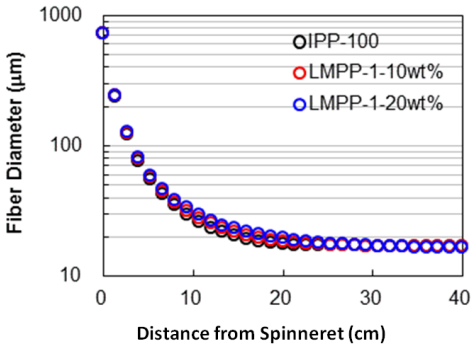

FIGURE 8.Fiber diameter profiles of IPP/LMPP blends

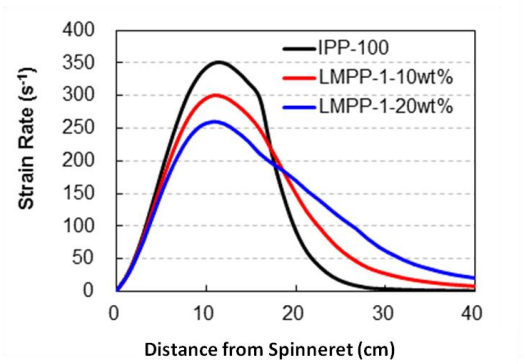

FIGURE 9. Strain rate profiles of IPP/LMPP blends

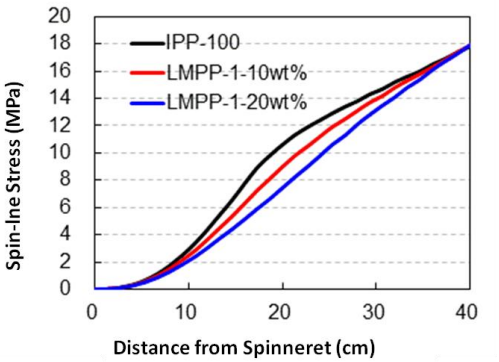

Figure 10. Spin-line stress of IPP/LMPP blends

3.3 Blending Effect of LMPP on Nonwoven Fabrics

Figure 11 shows the stress vs strain curve of non-woven fabrics of basis weight 15gsm. When the throughput per hole decreased to produce fine fiber of 1.1 denier, the tensile strength and elongation at break on both MD and TD increased remarkably.

It is considered that as the high speed spinning was possible by blending LMPP with PP to produce fine fibers, the number of fibers with melt bonds at the emboss increased and binding force between fibers in spunbond fabrics increased.

Figure 12 shows the results of softness for non-woven fabrics by the Cantilever test. The non-woven fabrics blending LMPP have low resistance force and softness. This result means the improved softness was obtained by thinning fibers and could produce non-woven fabrics with both softness and high strength.

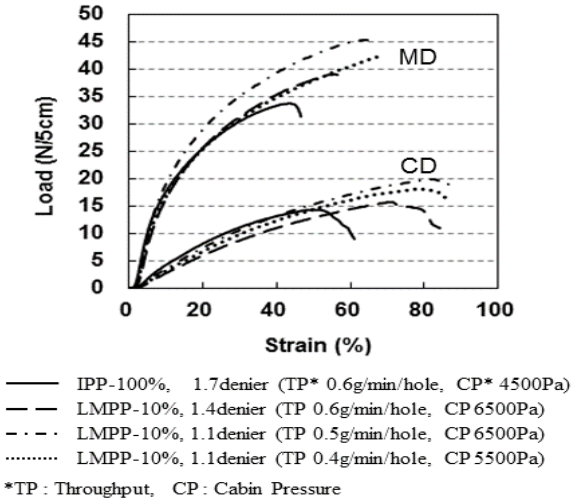

FIGURE 11. Load-Strain curve in MD and CD for multilayer nonwoven fabrics (three layer Spunbonds).

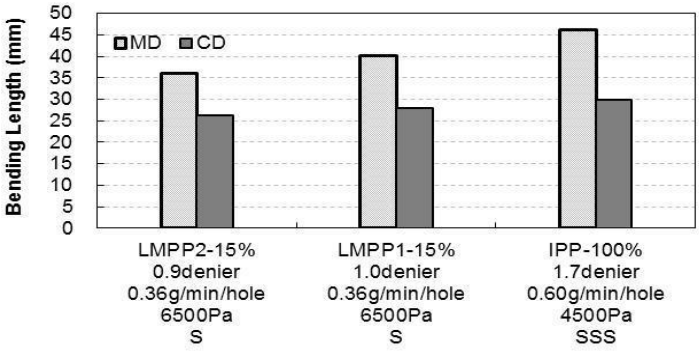

FIGURE 12. Cantilever test of nonwoven fabrics (Smaller bending length means nonwoven is softer)

REFERENCES

1) Y.Kohri, W.Takarada, H.Ito, T.Takebe, Y.Minami, T.Kanai, T.Kikutani, Seikei-Kakou, 20, 831 (2008)
2) T.Takebe, Y.Minami, T.Kanai, Seikei-Kakou, 21,(4) 202-207(2009)
3) N.Okumura, H.Ito, T.Kikutani, T.Kanai, Polymer Processing Society Annual Meeting-21 (2005)
4) Y.Kohri, T.Takebe, T.Kanai, T.Kikutani, Seikei-Kakou'14, Annual Meeting Proceedings (2014)
5) Y.Kohri, T.Takebe, Y.Minami, T.Kanai, W.Takarada, T.Kikutani, J. Polym. Eng., 35, 277-285(2015)